Supplemental Online Content

Loughnan R, Ahern J, Tompkins C, et al. Association of genetic variant linked to hemochromatosis with brain magnetic resonance imaging measures of iron and movement disorders. *JAMA Neurol*. Published online August 1, 2022. doi:10.1001/jamaneurol.2022.2030

This supplemental material has been provided by the authors to give readers additional information about their work.

eMethods

Neuroimaging Analysis

Atlas Registration

To allow for voxel-wise analysis, subjects' imaging data were aligned using a multimodal nonlinear elastic registration algorithm. At the end of the preprocessing steps outlined in *Image Processing* and described in detail in Hagler et al. [1], subjects' structural images and diffusion parameter maps were aligned to a UK Biobank-specific atlas, using a custom diffeomorphic registration method.

Labeling regions of interest (ROI)

Subcortical structures were labeled using Freesurfer 5.3[2]. Subjects' native space Freesurfer parcellations were warped to the atlas space and averaged across subjects. Additional subcortical nuclei, not available in the FreeSurfer segmentation, were labeled by registering readily available, downloadable, high spatial resolution atlases to our atlas space. The Pauli atlas was generated using T1 and T2 scans from 168 typical adults from the Human Connectome Project (HCP)[3]. The Najdenovska thalamic nuclei atlas was generated using a k-means algorithm taking as inputs mean fiber orientation density spherical harmonic coefficients from within a Freesurfer parcellation of the thalamus, using adult HCP data from 70 subjects[4]. All subcortical ROIs and abbreviations are listed in eTable 1.

Covariate Matched Controls

For the neuroimaging analysis we found matched controls on age, sex, scanner, mean cortical area, and top ten components of genetic ancestry. These matched controls were generated from the sample of 165 individuals with qualified imaging by fitting a logistic model to predict p.C282Y homozygosity from the listed covariates and then generating propensity scores[5] for each individual. Controls were selected based on propensity scores with a threshold of $|s_1 - s_2| \leq threshold$, where s_1 and s_2 were the respective propensity scores of a p.C282Y homozygote and their matched control, using a threshold of 1.5×10^{-4}. We performed this procedure using the *pymatch* library (version 0.3.1) in python[6].

Sex Stratified Analysis

In the covariate matched T2-weighted subsample described in Table 1 we performed sex-stratified analysis as described in the main (without sex as a fixed covariate) for T2-weighted images. This resulted in a male sample of 312 (64 p.C282Y homozygotes) individuals and a female sample of 437 females (90 p.C282Y homozygotes). eFigure 4 and eFigure 5 show results from this analysis.

C282Y Heterozygote Analysis

As transferrin saturations have also previously been shown to be higher in p.C282Y *heterozygote* individuals we performed additional analysis to investigate any effect of iron load on MRI scans and on risk for neurological disease. With there being a much higher proportion of individuals being heterozygote vs homozygote for p.C282Y we did find matched controls for this neuroimaging analysis as we did not deem there to be a very large imbalance between cases and controls. For the neuroimaging analysis this yielded 3,788 p.C282Y heterozygotes (1,879 male) and 22,705 controls (10,895 male) - i.e. individuals with no p.C282Y mutations).

Estimation of Mean Iron Accumulation Across Affected Brain Regions

To estimate mean iron concentration increases for p.C282Y homozygotes we calculated the mean beta estimates across voxels with ($p<10^{-5}$) for our R2* analysis – sample shown in Table 1 and results are shown in eFigure 3 . This beta value was then converted to units of Hz to an estimate of iron concentration using the conversion discussed in the main.

To estimate this same value for p.C282Y heterozygotes we performed, in the same T2*/R2* subsample described in the main, except excluding p.C282Y homozygotes. This resulted in 98 p.C282Y heterozygotes (43 male) and 438 controls (180 male). We then calculated voxel wise beta estimates (residualized for covariates, including sex) associating R2* voxelwise intensity with p.C282Y heterozygosity status. We then computed the mean beta estimate across $p<10^{-5}$ voxels identified in the R2* p.C282Y homozygote results shown in eFigure 3, to

ensure comparison across analogous regions. Once again this beta values was converted estimated iron levels as described in main methods.

Age Trajectories of T2-Weighted Intensities

With regional iron accumulation occurring in the human brain across the lifespan[7], we wanted to investigate if C282Y homozygotes showed a differential age trajectory for iron load as measured in T2-weighted MRI scans. To achieve this we extracted mean values, residualized for sex, scanner and top ten genetic PCs, across significant voxels ($p<10^{-5}$) for the analysis in main (Figure 2) from T2-weighted MRI scans for all individuals with qualified imaging (not subsampled for matched controls). This resulted in 155 C282Y homozygotes, 3,796 C282Y heterozygotes and 22,905 wildtypes (i.e. those with no C282Y mutations). We then fit lowess models for each genotype group of these mean T2-weighted values against age at scan, to plot the age resolved iron load effect.

Neurological Disease Burden Analysis

C282Y Heterozygote Analysis

We tested for an effect of C282Y heterozygosity on the same disorders as in the main (see Neurological Disease Burden Analysis) excluding p.C282Y homozygotes from this portion of the analysis. This yielded 65,315 p.C282Y heterozgytoes (29,935 male) and 420,084 controls (192,341 male) – i.e. those with no p.C282Y mutations. These models were employed in same way as described in the main.

eFigure 9,

eTable 4 and

eTable 5 show the results from this analysis.

Neuroimaging Association with Clinical Outcomes

We tested to if iron load (as measured by T2-weighted MRI intensity) related to risk for neurological disorders tested in the main analysis for C282Y homozygotes. To do this we extracted residualized mean T2-weighted intensity values for 14 regions for the 154 homozygotes with qualified imaging and plotted this against neurological disorder diagnosis status (Movement and Other Disorders of the Nervous System [G20-26] or [G90-99]) -

eFigure 10. P values were calculated by performing a Wilcoxon rank-sum test.

eResults

T2* Neuroimaging analysis

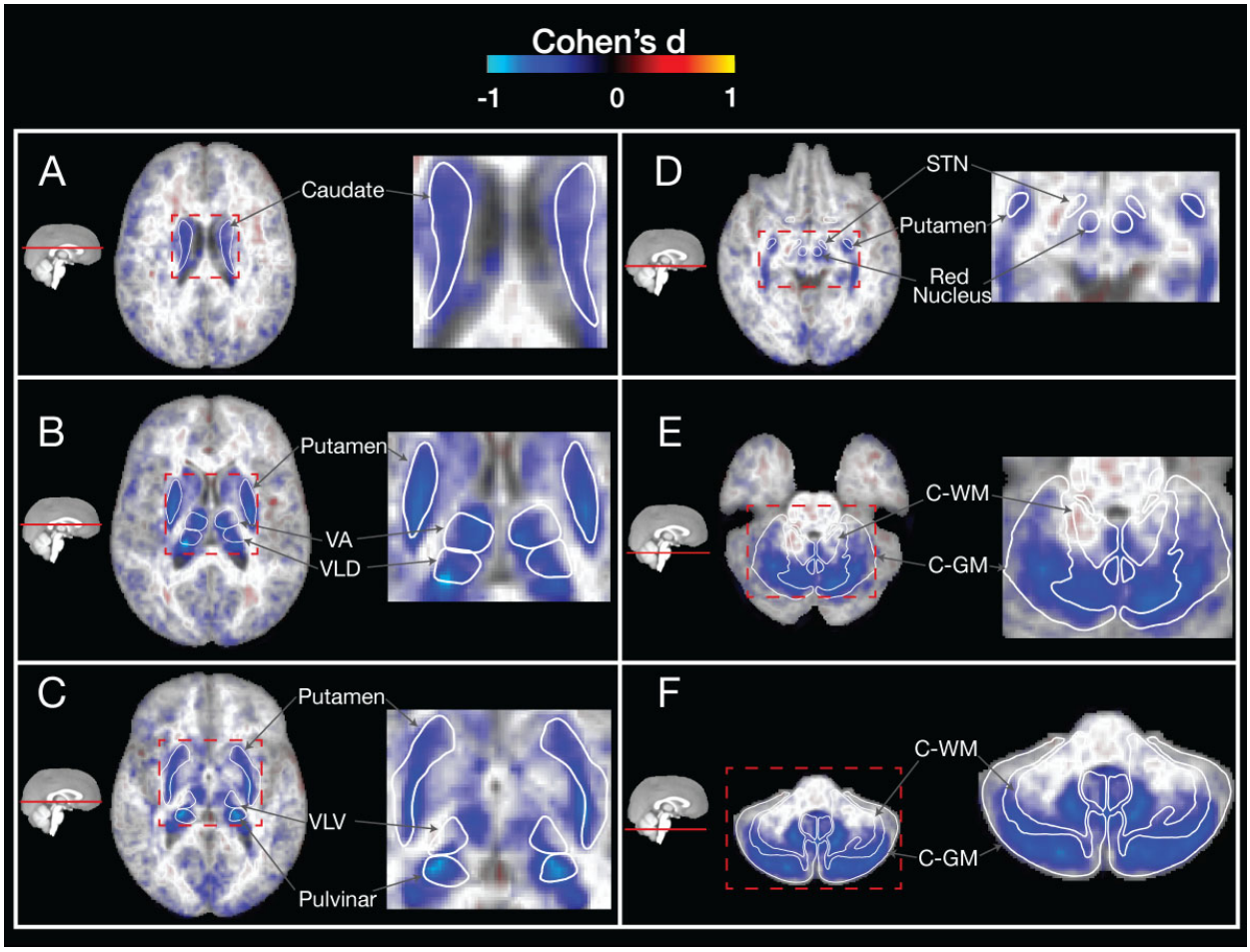

*eFigure 1 Voxelwise associations (Cohen's d) of **T2*** intensities between matched controls vs p.C282Y homozygote individuals. Blue regions represent lower **T2*** intensities (indicating higher iron deposition) for p.C282Y homozygotes. Lower **T2*** intensities are observed for p.C282Y homozygotes in the A. caudate nucleus, B. putamen, ventral anterior and ventral lateral dorsal nuclei of the thalamus, C. pulvinar nuclei of the thalamus. Large effects in D. subthalamic nucleus, red nucleus and E. cerebellum white matter were not seen as were observed for T2-weighted associations (compare with respective panels in Figure 2).*

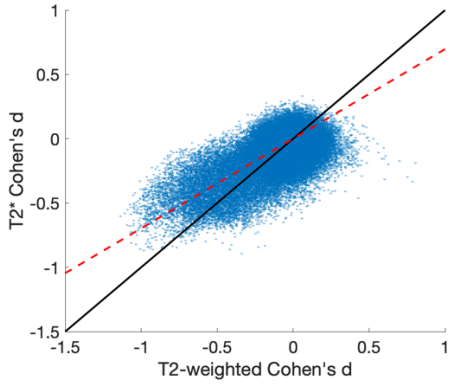

eFigure 2 Comparison of T2-weighted and T2 voxel intensity association with C282Y homozygosity as scatter plot – each point represents a single voxel. Black line indicates y=x (i.e. equal effect sizes). Red line indicates best fitting line (for points of at least moderate effects $x^2 + y^2 > 0.2$), $\beta = 0.70$ indicating approximately a 30% reduction in effect sizes observed in T2* vs T2-weighted associations.*

R2* Estimated Betas and Iron Concentration

eFigure 3 shows the beta estimates associating R2* intensity with p.C282Y homozygosity status. Calculating the mean across voxels with $p<10^{-5}$ yields an average iron concentration increase of 30.00 (µg/g dry). Performing the analogous association for p.C282Y heterozygotes yields an average estimated iron increase across the same voxels of 4.93 (µg/g dry).

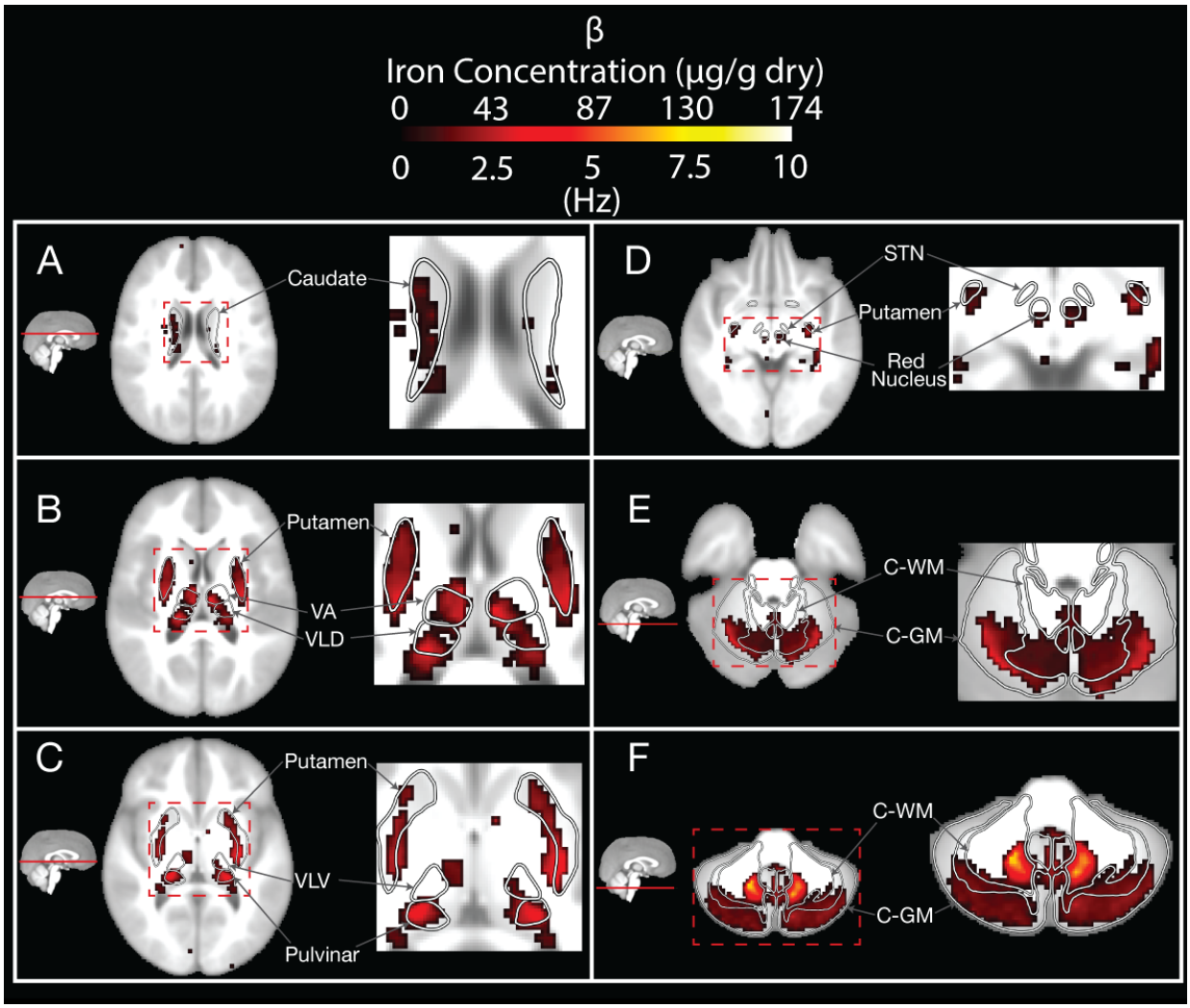

eFigure 3 Voxelwise beta estimates associating R2 (1/T2*) with C282Y homozygosity status. Only displaying voxels where $p<10^{-5}$. As R2* is directly proportional to iron concentration beta estimates are expressed both in units of Hz and as iron concentration differences between controls and C282Y homozygotes – see methods. Peak differences are observed in the pulvinar nucleus and the cerebellum white matter (C-WM). Mean iron increase across $p<10^{-5}$ voxels is 30.00(µg/g dry).*

Sex Stratified T2-Weighted Neuroimaging Analysis

Sex stratified results, eFigure 4, reveal a largely overlapping pattern of associations for males and females, although with larger effect sizes on average in males. By directly comparing effect sizes, eFigure 5, we estimate that effect sizes are 28% smaller in females vs males.

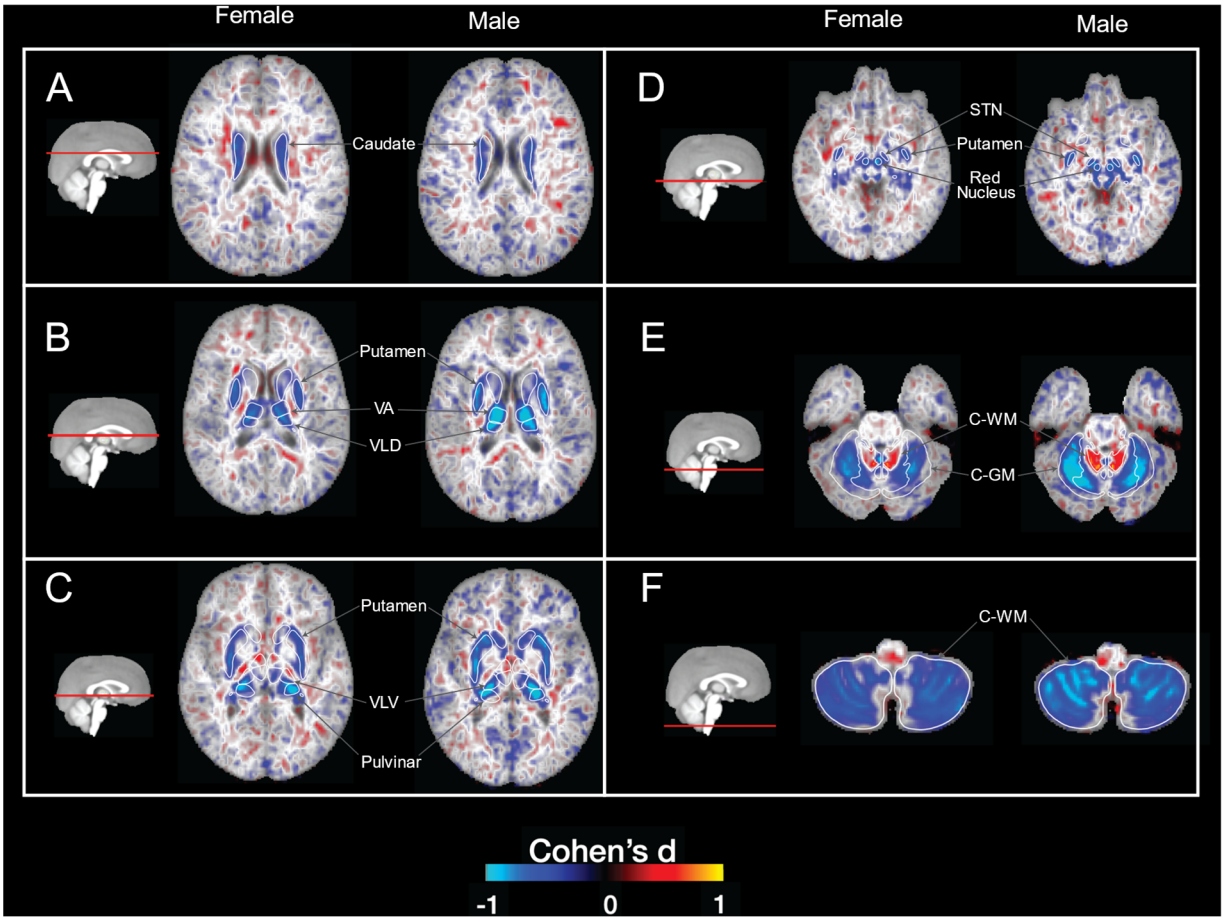

eFigure 4 Maps of sex stratified associations of p.C282Y homozygosity and T2 voxel intensities (Cohen's d). Overall effects are larger in males vs females, with largest effects in males observed in the VA, VLD and pulvinar nuclei of the thalamus (B) as well as in the C-WM and C-GM (E). Abbreviations: VA – ventral anterior, VLD – ventral anterior dorsal, VLV – ventral anterior ventral, C-WM – cerebellum white matter, C-GM – cerebellum GM.

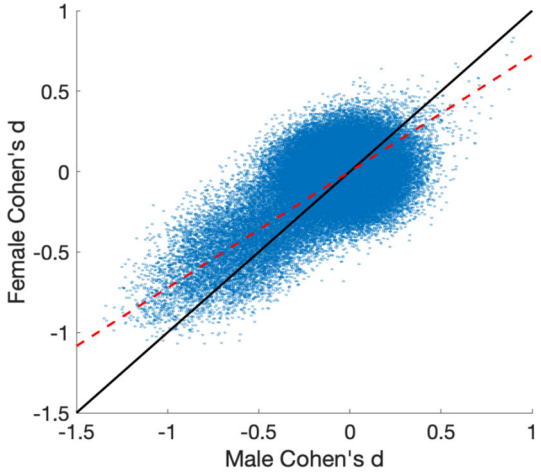

eFigure 5 Sex stratified associations of p.C282Y homozygosity and T2 voxel intensities (Cohen's d), as scatter plot – each point represents a single voxel. Black line indicates y=x (i.e. equal effect sizes). Red line indicates best fitting line (for points of at least moderate effects $x^2 + y^2 > 0.2$), $\beta = 0.72$ indicating approximately a 28% reduction in T2 intensity brain associations for females compared to males.

Neuroimaging Associations for p.C282Y Heterozygotes

eFigure 6 shows the voxelwise association of p.C282Y heterozygosity with T2-weighed intensities. Comparing this to Figure 2 from the main the location and direction of effects is very similar and is still highly significant, however with markedly reduced effect sizes.

eFigure 7 compares voxelwise effect sizes from Figure 2 and

eFigure 6, the best fit line indicates that the T2-weighted intensity effect is on average 82% lower for p.C282Y heterozygotes vs p.C282Y homozygotes.

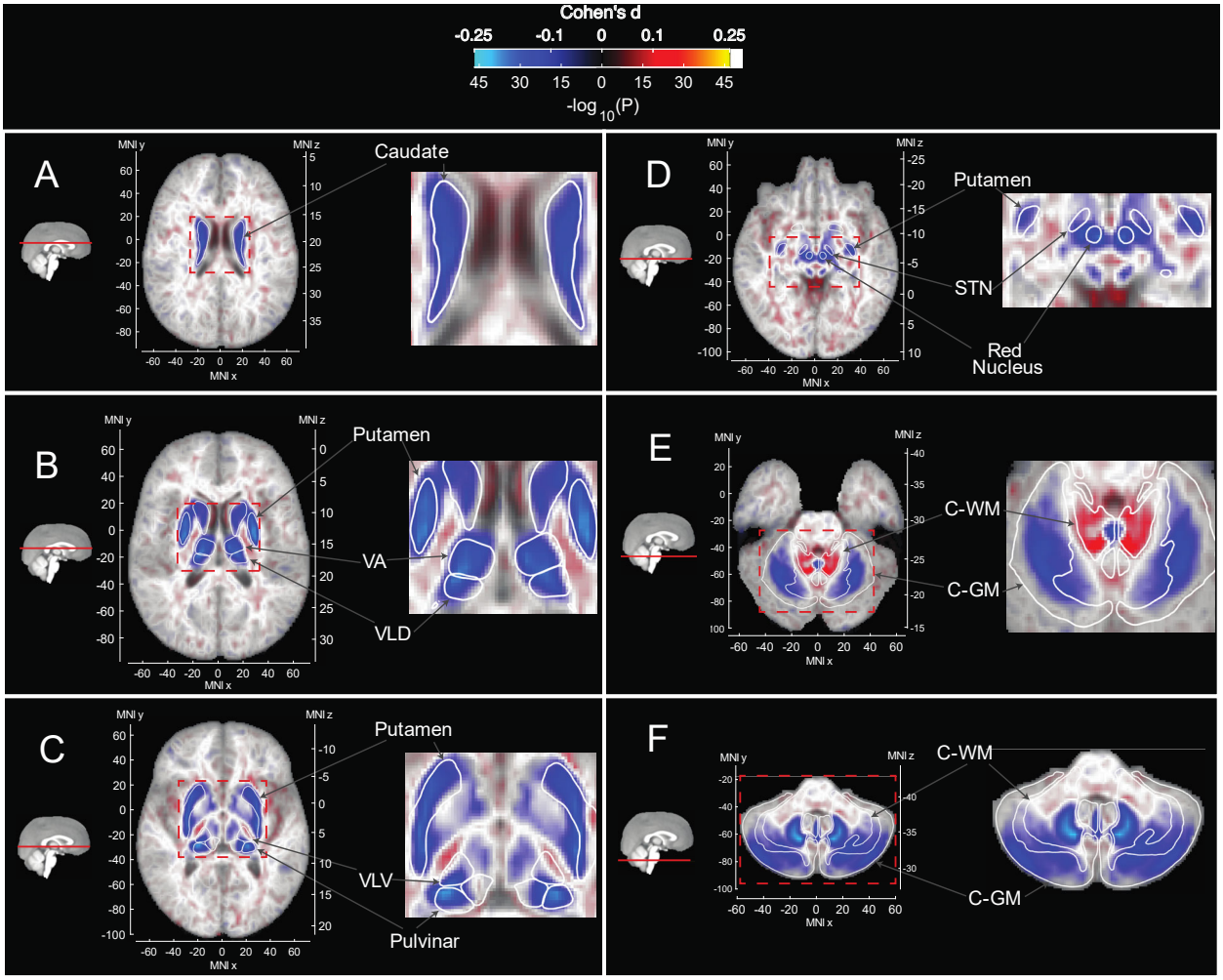

eFigure 6 Voxelwise associations (Cohen's d) of T2-weighted intensities in p.C282Y heterozygote individuals compared to controls (individuals with no p.C282Y mutations). Blue regions represent lower T2-weighted intensities for p.C282Y heterozygotes. Lower T2-weighted intensities are observed for p.C282Y heterozygotes in the A. caudate nucleus, B. putamen, ventral anterior and ventral-lateral dorsal nuclei of the thalamus, C. ventral-lateral ventral and pulvinar nuclei of the thalamus, D. red nucleus, sub-thalamic nucleus, E. and F. the cerebellum particularly the dentate nucleus. Higher T2-weighted intensities are observed in E. in the superior cerebellar peduncle (primary output pathway connecting the cerebellum to the thalamus and red nucleus). Note: the relatively lower p-values in relation to the main analysis (Figure 2) is due to the substantially larger sample size in this analysis.

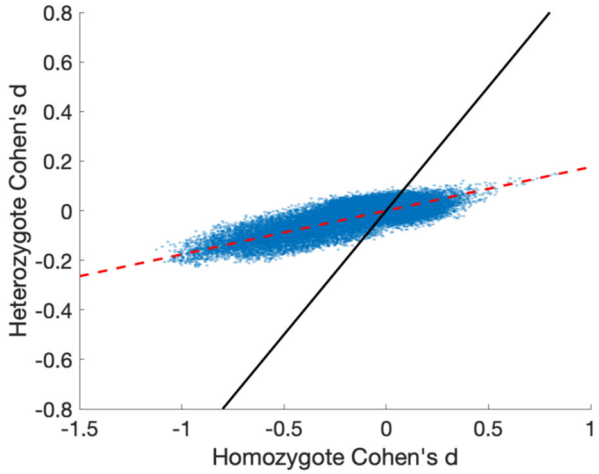

eFigure 7 Comparison of p.C282Y homozygote vs heterozygote voxelwise T2-weighted intensity effect (Cohen's d), as scatter plot. Each point represents a single voxel. Black line indicates y=x (i.e. equal effect sizes). Red line indicates best fitting line (for points of at least moderate effects $x^2 + y^2 > 0.2$), $\beta = 0.18$ indicating approximately a 82% reduction in T2-weighted intensity brain associations for p.C282Y heterozygotes vs homozygotes.

Age Trajectories of T2-Weighted Intensities

eFigure 8 shows T2-weighted intensity age trajectories for each C282Y genotype group with only individual datapoints for the C282Y homozygotes being shown to avoid overcrowding. Across the agespan of this sample C282Y homozgygotes appear to show lower mean T2-weighted intensities (indicating more iron deposition), with a apparent accelerated iron accumulation in later years (>70 years) compared to heterozygotes and wildtypes (those with no C282Y mutations) – although this should be interpreted with caution given the modest sample size in this age range.

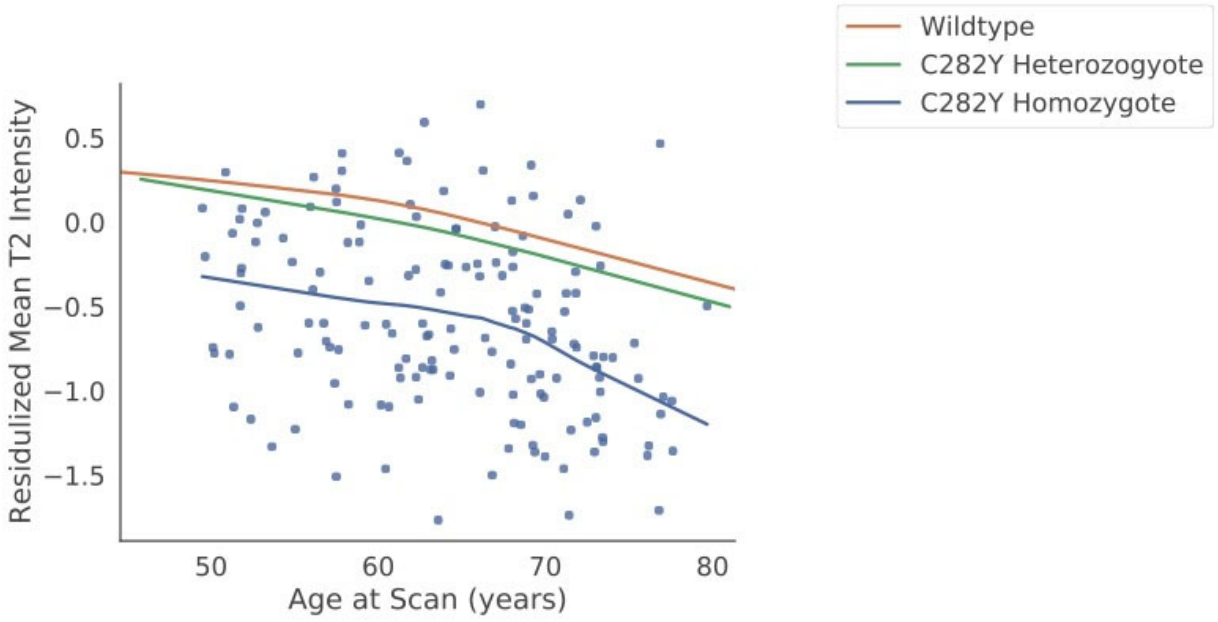

eFigure 8 Age moderation of mean T2-weighted values for voxels where $p<10^{-5}$ in Figure 2 from main. Lines represent lowess fits for each genotype group.

Neurological Disease Burden for p.C282Y Heterozygotes

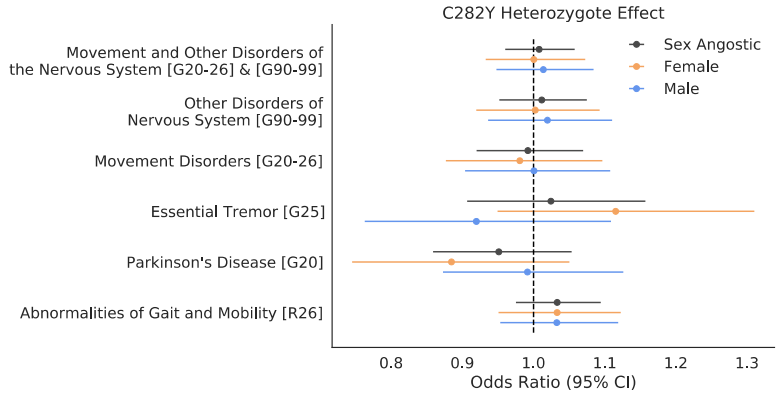

	Odds Ratio (95% CI)		
	Sex Agnostic	Female	Male
Movement and Other Disorders of the Nervous System [G20-26] & [G90-99]	1.01 (0.96 to 1.06)	1.00 (0.93 to 1.07)	1.01 (0.95 to 1.08)
Other Disorders of Nervous System [G90-99]	1.01 (0.95 to 1.07)	1.00 (0.92 to 1.09)	1.02 (0.94 to 1.11)
Movement Disorders [G20-26]	0.99 (0.92 to 1.07)	0.98 (0.88 to 1.10)	1.00 (0.90 to 1.11)
Essential Tremor [G25]	1.02 (0.91 to 1.16)	1.12 (0.95 to 1.31)	0.92 (0.76 to 1.11)
Parkinson's Disease [G20]	0.95 (0.86 to 1.05)	0.88 (0.75 to 1.05)	0.99 (0.87 to 1.13)
Abnormalities of Gait and Mobility [R26]	1.03 (0.98 to 1.09)	1.03 (0.95 to 1.12)	1.03 (0.95 to 1.12)

eFigure 9 Sex agnostic and sex-stratified effect of C282Y heterozygosity for neurological disorders (y-axis), values in square brackets indicate ICD10 codes or ranges of ICD10 codes for categories of diagnoses. The dotted vertical line indicates an odds ratio of 1 i.e., null effect.

Neuroimaging Association with Clinical Outcomes

Interpreting these results with caution, given the small sample size, there appears to be no relationship between T2-weighted intensities in these regions. This may be consistent with other secondary disorders of hemochromatosis that appear to show some individuals present with a high iron load and no clinical manifestations[8] – this could be due to other environmental or genetic attributes providing a moderating effect.

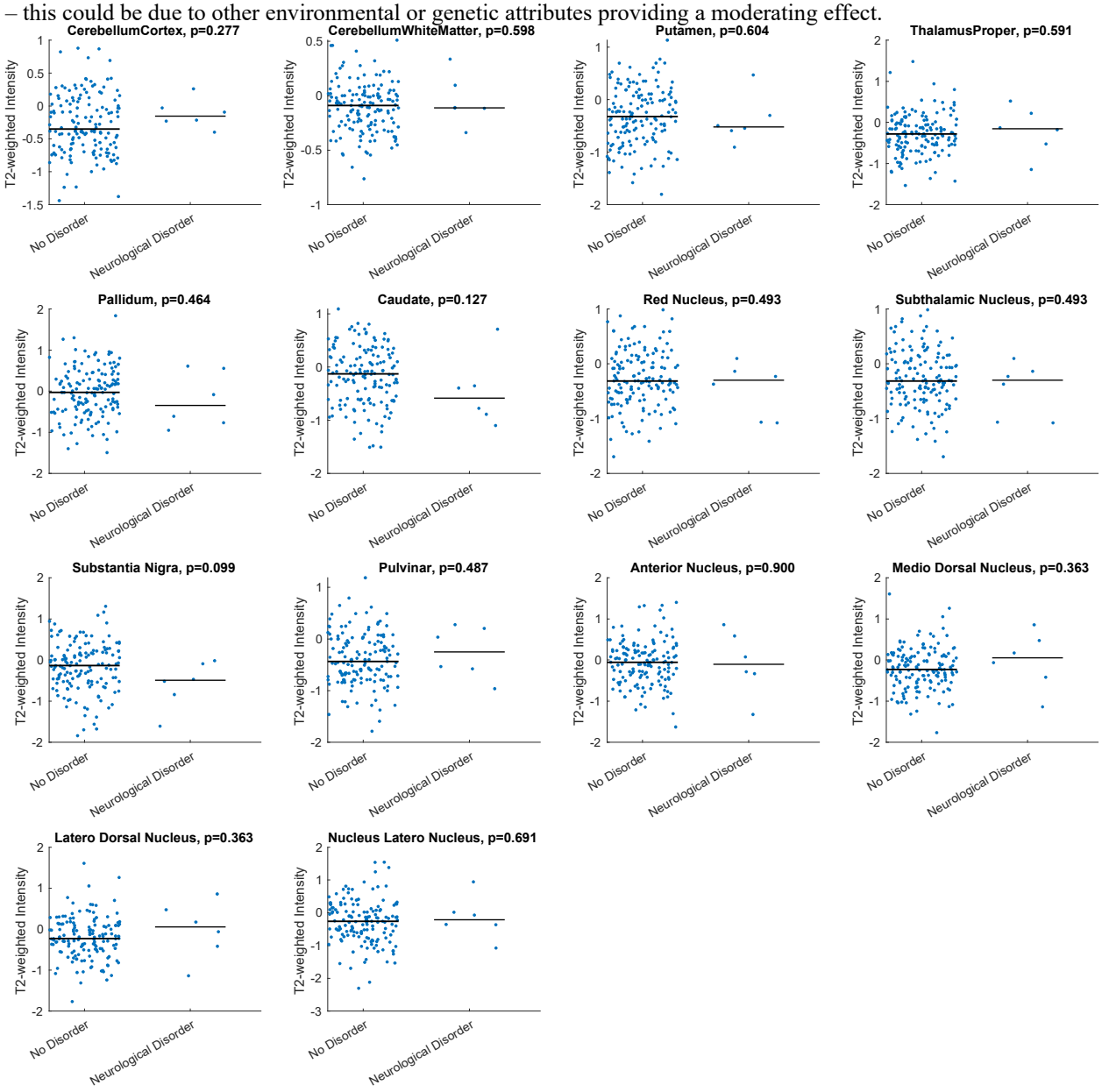

eFigure 10 Mean T2-weighted intensity values for 154 C282Y homozygotes vs diagnosis status for any neurological disorder (Movement and Other Disorders of the Nervous System [G20-26] or [G90-99]). Solid horizontal lines indicate median values for each group.

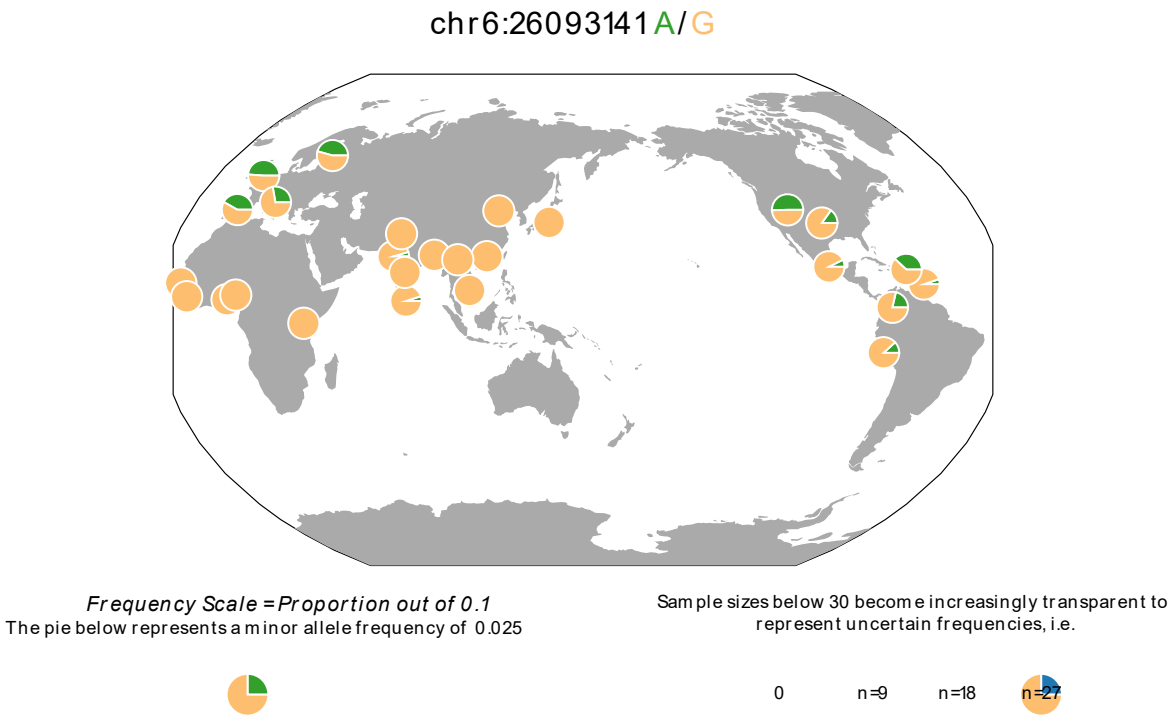

eFigure 11 Global distribution of p.C282Y (rs1800562). Allele frequencies are highest in Europe (particularly northern Europe) and parts of north America. Map generated from the Geography of Genetic Variants Browser[9].

FreeSurfer 5.3 segmentation T1	Pauli, 2018 HCP T1 & T2	Najdenovska, 2018 HCP FODs
Amygdala (Amg)	Putamen (Pu)	Anterior (tA)
Hippocampus (Hipp)	Caudate (Ca)	Ventral anterior (tVA)
Putamen (Pu)	Nucleus accumbens (NAcc)	Mediodorsal (tMD)
Caudate (Ca)	Extended amygdala (EA)	Ventral-latero-ventral (tVLV)
Globus pallidus (GP)	Substantia nigra pars compacta (SNpc)	Ventral-latero-dorsal (tVLD)
Accumbens area (NAcc)	Substantia nigra pars reticulata (SNpr)	Central-latero-lateral-posterior-medial-pulvinar (tC)
Thalamus (Thal)	Red nucleus (RN)	Pulvinar (tP)
Ventral Diencephalon (VDC)	Parabrachial pigmented nucleus (PBP)	
	Hypothalamus (Hyp)	
	Mamillary nucleus (MN)	
	Subthalamic nucleus (STN)	

eTable 1 ***Regions of interest (ROIs) labelled using 3 different methods.*** *Column 1) automatic segmentation using FreeSurfer 5.3 applied to each subject's T1 image in atlas space[2]; Column 2) registration of the Pauli atlas of subcortical nuclei to the multispectral atlas[3]; Column 3) registration of the the Najdenovska thalamic nuclei atlas to our data[4].*

Diagnosis	Total Controls	Total Cases	C282Y Cases	OR	CI_lower	CI_upper	P
Abnormalities of Gait and Mobility [R26]	478166	10122	64	1.0266	0.7995	1.3182	0.83680
Parkinson's Disease [G20]	484970	3318	29	1.4391	0.9946	2.0822	0.05343
Essential Tremor [G25]	486086	2202	22	1.6430	1.0770	2.5065	0.02121
Movement Disorders [G20-26]	482307	5981	53	1.4618	1.1111	1.9232	0.00667
Other Disorders of Nervous System [G90-99]	479012	9276	65	1.1908	0.9300	1.5246	0.16614
Movement and Other Disorders of the Nervous System [G20-26] & [G90-99]	473539	14749	113	1.2921	1.0690	1.5618	0.00805

eTable 2 Sex agnostic regression tables results for associating C282Y homozygote (+/+) cases with diagnoses of different neurological disorders. Models were fit for males and females together, with sex as a fixed effect.

Male							
Diagnosis	**Total Controls**	**Total Cases**	**C282Y Cases**	**OR**	**CI_lower**	**CI_upper**	**P**
Abnormalities of Gait and Mobility [R26]	218350	5219	28	0.8960	0.6142	1.3072	0.56878
Parkinson's Disease [G20]	221495	2074	22	1.8270	1.1921	2.7999	0.00566
Essential Tremor [G25]	222557	1012	12	2.0202	1.1388	3.5840	0.01621
Movement Disorders [G20-26]	220322	3247	34	1.8049	1.2783	2.5485	0.00079
Other Disorders of Nervous System [G90-99]	218903	4666	37	1.3912	1.0012	1.9331	0.04915
Movement and Other Disorders of the Nervous System [G20-26] & [G90-99]	215938	7631	68	1.5677	1.2249	2.0064	0.00036

Female							
Diagnosis	**Total Controls**	**Total Cases**	**C282Y Cases**	**OR**	**CI_lower**	**CI_upper**	**P**
Abnormalities of Gait and Mobility [R26]	259816	4903	36	1.1541	0.8269	1.6109	0.39948
Parkinson's Disease [G20]	263475	1244	7	0.8713	0.4132	1.8374	0.71746
Essential Tremor [G25]	263529	1190	10	1.3366	0.7152	2.4976	0.36316
Movement Disorders [G20-26]	261985	2734	19	1.0975	0.6962	1.7302	0.68861
Other Disorders of Nervous System [G90-99]	260109	4610	28	1.0032	0.6894	1.4600	0.98649
Movement and Other Disorders of the Nervous System [G20-26] & [G90-99]	257601	7118	45	1.0269	0.7624	1.3834	0.86113

eTable 3 Sex stratified regression tables results for associating C282Y homozygote (+/+) cases with diagnoses of different neurological disorders. Models were fit separately for males and females.

Diagnosis	Total Controls	Total Cases	C282Y Cases	OR	CI_lower	CI_upper	P
Abnormalities of Gait and Mobility [R26]	475341	10058	1404	1.0333	0.9753	1.0946	0.26631
Parkinson's Disease [G20]	482110	3289	433	0.9513	0.8588	1.0537	0.33809
Essential Tremor [G25]	483219	2180	305	1.0245	0.9068	1.1574	0.69779
Movement Disorders [G20-26]	479471	5928	807	0.9921	0.9201	1.0697	0.83613
Other Disorders of Nervous System [G90-99]	476188	9211	1248	1.0116	0.9520	1.0749	0.70947
Movement and Other Disorders of the Nervous System [G20-26] & [G90-99]	470763	14636	1993	1.0079	0.9603	1.0579	0.74961

eTable 4 Sex agnostic regression tables results for associating C282Y heterozygotes (+/-) cases with diagnoses of different neurological disorders. Controls were individuals with no C282Y mutations (-/-). Models were fit for males and females together, with sex as a fixed effect.

Male							
Diagnosis	**Total Controls**	**Total Cases**	**C282Y Cases**	**OR**	**CI_lower**	**CI_upper**	**P**
Abnormalities of Gait and Mobility [R26]	217085	5191	731	1.0327	0.9532	1.1190	0.43100
Parkinson's Disease [G20]	220224	2052	282	0.9915	0.8729	1.1262	0.89549
Essential Tremor [G25]	221276	1000	128	0.9197	0.7628	1.1089	0.38048
Movement Disorders [G20-26]	219063	3213	444	1.0006	0.9037	1.1079	0.99032
Other Disorders of Nervous System [G90-99]	217647	4629	634	1.0196	0.9362	1.1105	0.65534
Movement and Other Disorders of the Nervous System [G20-26] & [G90-99]	214713	7563	1041	1.0138	0.9479	1.0844	0.68848

Female							
Diagnosis	**Total Controls**	**Total Cases**	**C282Y Cases**	**OR**	**CI_lower**	**CI_upper**	**P**
Abnormalities of Gait and Mobility [R26]	258256	4867	673	1.0332	0.9508	1.1227	0.44092
Parkinson's Disease [G20]	261886	1237	151	0.8848	0.7452	1.0505	0.16221
Essential Tremor [G25]	261943	1180	177	1.1155	0.9495	1.3104	0.18356
Movement Disorders [G20-26]	260408	2715	363	0.9807	0.8770	1.0968	0.73334
Other Disorders of Nervous System [G90-99]	258541	4582	614	1.0025	0.9196	1.0930	0.95410
Movement and Other Disorders of the Nervous System [G20-26] & [G90-99]	256050	7073	952	1.0004	0.9330	1.0727	0.99051

eTable 5 Sex stratified regression tables results for associating C282Y heterozygotes (+/-) cases with diagnoses of different neurological disorders. Controls were individuals with no C282Y mutations (-/-). Models were fit separately for males and females.

eReferences

1. Hagler DJ, Hatton SN, Cornejo MD, et al. Image processing and analysis methods for the Adolescent Brain Cognitive Development Study. *Neuroimage*. 2019;202(August). doi:10.1016/j.neuroimage.2019.116091
2. Fischl B, Salat DH, Busa E, et al. Whole brain segmentation: Automated labeling of neuroanatomical structures in the human brain. *Neuron*. 2002;33(3):341-355. doi:10.1016/S0896-6273(02)00569-X
3. Pauli WM, Nili AN, Michael Tyszka J. Data Descriptor: A high-resolution probabilistic in vivo atlas of human subcortical brain nuclei. *Sci Data*. 2018;5:1-13. doi:10.1038/sdata.2018.63
4. Najdenovska E, Alemán-Gómez Y, Battistella G, et al. In-vivo probabilistic atlas of human thalamic nuclei based on diffusion-weighted magnetic resonance imaging. *Sci Data*. 2018;5(October):1-11. doi:10.1038/sdata.2018.270
5. Rosenbaum PR, Rubin DB. Constructing a control group using multivariate matched sampling methods that incorporate the propensity score. *Am Stat*. 1985;39(1):33-38. doi:10.1080/00031305.1985.10479383
6. Benmiroglio. pymatch. https://github.com/benmiroglio/pymatch.
7. Aquino D, Bizzi A, Grisoli M, et al. Age-related Iron Deposition in the Basal Ganglia : Quantitative Methods : Results : Conclusion : *Neuroradiology*. 2009;252(1):165-172.
8. Powell LW, Seckington RC, Deugnier Y. Haemochromatosis. *Lancet*. 2016;388(10045):706-716. doi:10.1016/S0140-6736(15)01315-X
9. Marcus JH, Novembre J. Visualizing the geography of genetic variants. *Bioinformatics*. 2017;33(4):594-595. doi:10.1093/bioinformatics/btw643